



Co-published by  
**Institute of Fluid-Flow Machinery**  
Polish Academy of Sciences  
**Committee on Thermodynamics and Combustion**  
Polish Academy of Sciences

Copyright©2024 by the Authors under license CC BY 4.0

<http://www.imp.gda.pl/archives-of-thermodynamics/>



# Evaluation of the effect of rotational speed and rheological nature on heat transfer of complex fluid between two cylinders

Abdeljalil Benmansour<sup>a</sup>, Housseem Laidoudi<sup>a\*</sup>

<sup>a</sup>Laboratory of Sciences and Marine Engineering, Faculty of Mechanical Engineering, USTO-MB, BP 1505, El-Menaouer, Oran, 31000, Algeria.

\*Corresponding author email: [housseem.laidoudi@univ-usto.dz](mailto:housseem.laidoudi@univ-usto.dz)

Received: 10.03.2023; revised: 27.05.2023; accepted: 06.12.2023

## Abstract

This paper presents numerical results for flow behavior between a cold inner cylinder and a hot outer cylinder. Both cylinders are placed horizontally. The space separating the two compartments is completely filled with a fluid of a complex rheological nature. In addition, the outer container is subjected to a constant and uniform rotational speed. The results of this work were obtained after solving the differential equations for momentum and energy. The parameters studied in this research are: the intensity of thermal buoyancy, the speed of rotation of the outer container and the rheological nature of the fluid. These elements are expressed mathematically by the following values: Richardson number ( $Ri = 0$  and  $1$ ), Reynolds number ( $Re = 1$  to  $40$ ), power-law number ( $n = 0.8, 1$  and  $1.4$ ) and Prandtl number ( $Pr = 50$ ). The results showed that the speed of rotation of the cylinder and the rheological nature of the fluids have an effective role in the process of heat transfer. For example, increasing the rotational speed of the enclosure and/or changing the nature of fluid from shear-thickening into shear-thinning fluid improves the thermal transfer rate.

**Keywords:** Mixed convection; Rheological behavior; Steady simulation; CFD; Nusselt number

Vol. 45(2024), No. 1, 65–73; doi: 10.24425/ather.2024.150439

Cite this manuscript as: Benmansour, A. & Laidoudi, H. (2024). Evaluation of the effect of rotational speed and rheological nature on heat transfer of complex fluid between two cylinders. *Archives of Thermodynamics*. 45(1), 65–73.

## 1. Introduction

Numerical simulation has become one of the most important methods used in the study of complex fluids and heat transfer, due to its accuracy in calculation and saving time and money. This study is related to a huge range of engineering and industrial applications, among which we mainly mention: irrigation and water treatment techniques, thermal mechanics, chemical industries and others. Through numerical simulations, we can predict the thermodynamic behaviour of a fluid in any proposed geometry. This allows access to the calculation of some important coefficients in engineering applications such as the drag

coefficient and average Nusselt number.

Recently, there have been many studies concerning the rate of heat transfer between two cylinders, by applying a set of conditions and elements. Chatterjee and Halder [1, 2] studied the free convection between two rotating cylinders and a square enclosure. The MHD effect was added to the system. The control of physical parameters was by the dimensionless number of  $Ra$ ,  $Re$  and  $Ha$ . The results proved that these parameters have an influence on the heat transfer.

In general, if the case of the movement of fluid particles is only the force of gravity, then this type of heat transfer is called

## Nomenclature

$a$	– small dimension of inner cylinder, m
$b$	– big dimension of inner cylinder, m
$D$	– diameter of the outer enclosure, m
$g$	– gravitational acceleration, $\text{m/s}^2$
$n_s$	– normal vector
$Nu$	– Nusselt number
$p$	– pressure, $\text{N/m}^2$
$p^*$	– dimensionless pressure
$Pr$	– Prandtl number
$Ri$	– Richardson number
$T$	– temperature, K
$u$	– dimensional velocity component in $x$ -direction, m/s
$u^*$	– dimensionless velocity component in $x$ -direction
$v$	– dimensional velocity component in $y$ -direction, m/s
$v^*$	– dimensionless velocity component in $y$ -direction

$x$	– dimensional coordinate in horizontal direction, m
$x^*$	– dimensionless coordinate in horizontal direction
$y$	– dimensional coordinate in vertical direction, m
$y^*$	– dimensionless coordinate in vertical direction

## Greek symbols

$\alpha$	– thermal diffusivity, $\text{Pa}\cdot\text{s}$
$\beta_T$	– coefficient of thermal expansion, $\text{K}^{-1}$
$\mu$	– dynamic viscosity, $\text{Pa}\cdot\text{s}$
$\nu$	– kinematic viscosity, $\text{m}^2/\text{s}$
$\rho$	– density, $\text{kg/m}^3$

## Subscripts and Superscripts

$c$	– cold
$h$	– heat
$l$	– local

natural as it has been studied by many researchers [3–5]. In this natural convection mode, some researchers have studied the effect of the geometric shape of the system [6–8], while others focused on the effect of fluid properties [9–11], another group of researchers was interested in studying the effect of gradual conditions [12–14]. Whereas if the cause is due to an external engine that pushes the fluid causing it to move, then in this case it is called thermal transfer by forced convective mode [15–17]. In this mode, some researchers studied the effect of flow velocity [18–20], others tested the effectiveness of the fluid in terms of heat transfer [21–23], and others touched on testing the effect of the geometrical configuration of the system [24, 25]. Finally, if they meet together, as is in our work, the type of heat transfer becomes a mixture, that is the natural type and the forced type at the same time [26–28]. This last mode of heat transfer is called also mixed convection [29–31]. In this type, the essential factors under examination are: the fluid velocity [32–34] and the intensity of thermal buoyancy force [35].

Laidoudi and Ameer [36] studied the mixed convection of power-law fluids between two rotating obstacles. The governing parameters here were:  $Re$ ,  $Ri$ ,  $n$  and the rotational direction of both cylinders. It was found that when the obstacles rotate in the same direction the heat transfer becomes negligible. Laidoudi and Ameer [37] also presented a numerical work about two fixed cylinders placed inside a big circular cylinder. This outer cylinder regularly rotated at uniform velocity. The arrangement of inner obstacles was taken into account. The results showed that the speed velocity of the outer obstacle, the power-law number and the arrangement of the inner obstacles influenced the rate of heat transfer inside the studied domain. There is also a set of ideas related to this type of research that can be included in this work [38–40]. There is also the effect of external factors on the mixed convection such as the magnetic field [41, 42].

After reviewing the complex fluids, it was found that they are defined by one mathematical model called the model of Ostwald. Indeed, this model combines the Newtonian fluid, shear-thinning fluid and shear-thickening fluid. In contrast, the mixed

convection heat transfer is controlled by the non-dimensional number called Richardson number ( $Ri$ ). This number gives the ratio of the effect of forced convection to the natural convection. So, when  $Ri = 0$ , there is only pure forced convection, but when  $Ri \neq 0$ , there are both effects of forced and free convection.

By following the latest research of heat transfer between two obstacles with the rotation of the outer one, it is clear that there are not many works, especially with the presence of different shapes of the inner cylinder. Therefore, this work is considered a continuation of what was done by researchers Laidoudi and Ameer [36]. That is, the work involves numerical simulations of a complex fluid enclosed between two horizontal cylinders. The outer obstacle is hot and rotates at a constant speed while the inner obstacle is cold and stationary. A new thing in the present research is that the geometric shape of the inner obstacle is different from the rest of the previous shapes. Other elements studied in this work are: the intensity of thermal buoyancy, the rheological nature of the fluid and the speed of rotation of the outer container.

The relationship between this work and the previous work of Laidoudi and Ameer [36] is that in the previous work, the inner cylinder has a high temperature and the outer cylinder is cold, while here this proposition has been reversed, making this work new and supplementary to the previous one. The results of this work can be used in many applications, including: thermal insulation systems, high-performance heat exchangers, cooling systems in solar panels and others. This work can also be used in academic work related to thermal science and fluid mechanics.

## 2. Studied domain

A simplified model of the domain studied is presented in Fig. 1. The studied space includes two cylinders of different shapes placed horizontally. The inner cylinder has a geometric form shaped like a rhombus while the outer cylinder has a circular shape. In addition, the outer enclosure undergoes rotation at a constant speed  $\omega$ . The outer cylinder is characterized by the diameter  $D$  while the interior is characterized by the dimensions  $a$

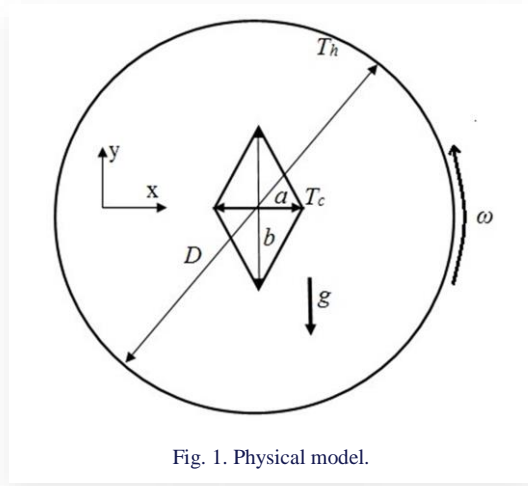


Fig. 1. Physical model.

and  $b$ . The values of these dimensions are given by the following ratios:  $b/D = 0.4$  and  $a/b = 0.5$ . As for the heat distribution, it is as follows: the outer cylinder wall has a high temperature  $T_h$ , while the inner cylinder has a low wall temperature  $T_c$ . These temperatures are uniform and constant along the walls. As for the volume between the external and internal cylinders, it is filled with a complex fluid. The value of its thermal constants is given by the Prandtl number ( $Pr = 50$ ) while the apparent dynamic viscosity is expressed by the Oswald model.

### 3. Mathematical formulation

The dynamic viscosity of this complex fluid is expressed as [36]:

$$\mu = m \left( \frac{I_2}{2} \right)^{\frac{n-1}{2}}, \quad (1)$$

where  $I_2$  is given as [36]:

$$\left( \frac{I_2}{2} \right) = 2 \left( \frac{\partial u}{\partial x} \right)^2 + 2 \left( \frac{\partial v}{\partial y} \right)^2 + \left( \frac{\partial u}{\partial x} + \frac{\partial v}{\partial y} \right)^2. \quad (2)$$

The governing dimensionless numbers of Prandtl, Reynolds and Richardson are expressed as [37]:

$$Pr = \frac{m c_p}{k \omega^{n-1}}, \quad (3)$$

$$Re = \frac{\rho (\omega D)^{2-n} D^n}{m}, \quad (4)$$

$$Ri = \frac{g \beta_T \Delta T D}{(\omega D)^2}, \quad (5)$$

where  $m$ ,  $c_p$ ,  $k$ ,  $\rho$ ,  $\omega$ ,  $\beta_T$ ,  $n$ , and  $g$  denote the consistency index, specific heat capacity, thermal conductivity of fluid, fluid density, rotational speed, volume expansion coefficient, power-law index and gravitational acceleration.

The Prandtl number  $Pr$  describes the thermo-physical properties of the working fluid for example 6.01 is for the water, the Reynolds number  $Re$  shows the rotational speed of the outer cylinder and the Richardson number  $Ri$  describes the ratio between the natural and forced convection [1], [2] and [31].

When  $n = 1$ , the fluid is Newtonian. When  $n = 1.4$ , the fluid is shear-thinning. When  $n = 0.8$ , the fluid is shear-thickening.

Furthermore, when  $Ri = 0$ , there is only a pure forced convection. For  $Ri = 1$ , the convection in this case is mixed. A Newtonian fluid ( $n = 1$ ) means that the dynamic viscosity of the fluid is independent of the flow velocity. A shear-thinning fluid ( $n < 1$ ) means that the higher the flow velocity, the lower the dynamic viscosity, whereas a shear-thickening fluid means that the higher the flow velocity, the higher the viscosity of the fluid.

The similarity numbers are placed in the basic equations of momentum and energy [1, 2] as follows:

$$\left( \frac{\partial u^*}{\partial x^*} \right) + \left( \frac{\partial v^*}{\partial y^*} \right) = 0, \quad (6)$$

$$u^* \frac{\partial u^*}{\partial x^*} + v^* \frac{\partial u^*}{\partial y^*} = -\frac{\partial p^*}{\partial x^*} + \frac{1}{Re} \left( \frac{\partial \tau_{xx}^*}{\partial x^*} + \frac{\partial \tau_{yy}^*}{\partial y^*} \right), \quad (7)$$

$$u^* \frac{\partial v^*}{\partial x^*} + v^* \frac{\partial v^*}{\partial y^*} = -\frac{\partial p^*}{\partial y^*} + \frac{1}{Re} \left( \frac{\partial \tau_{xy}^*}{\partial x^*} + \frac{\partial \tau_{yx}^*}{\partial y^*} \right) + Ri T^*, \quad (8)$$

$$u^* \frac{\partial T^*}{\partial x^*} + v^* \frac{\partial T^*}{\partial y^*} = \frac{1}{Pr Re} \left( \frac{\partial^2 T^*}{\partial x^{*2}} + \frac{\partial^2 T^*}{\partial y^{*2}} \right), \quad (9)$$

where dimensionless parameters are defined by the following expressions:

$$(u^*, v^*) = \frac{(u, v)}{\omega D}, p^* = \frac{p}{\rho (\omega D)^2}, T^* = \frac{(T - T_c)}{(T_h - T_c)}, \quad (10)$$

$$(x^*, y^*) = \frac{(x, y)}{D}, \tau^* = \frac{\tau}{m (\omega^n)}. \quad (11)$$

In the equations above, the symbol (\*) means the dimensionless quantities;  $x$  and  $y$  refer to the dimensions in the Cartesian coordinate system;  $u$  and  $v$  indicate the velocity components;  $p$  and  $T$  refer to the pressure and temperature, respectively,  $\omega$  indicates the rotational speed.

The expressions for the local and average Nusselt numbers are given as:

$$Nu_L = \left[ \frac{\partial T^*}{\partial n_s} \right], Nu = \frac{1}{A} \int Nu_L dA, \quad (12)$$

where  $n_s$  is the normal unit vector and  $A$  is the surface area.  $Nu$  is the average value of the local Nusselt number along the hot body.

The suitable boundary conditions for this domain are: for hydrodynamic conditions, no-slip condition with velocity components  $u = 0$ ,  $v = 0$  applied at the walls of inner and outer cylinders. Also, the outer enclosure has a rotating speed  $\omega$ . For the thermal condition, around the inner obstacle  $T = T_c$  and  $T = T_h$  is considered at the outer cylinder.

At the beginning, Eqs. (6–9) were solved in the dimensional form, after which changes were applied to the results using Eqs. (10) and (11).

### 4. Numerical procedure

The computational grid was created by Gambit. The final form of this grid is shown in Fig. 2. The grid elements are irregular with the elements being centred around the inner obstacle, where the calculation is very accurate and important. The grid consists of 9 912 elements. This number was considered after a study was conducted showing the effect of number of elements on the obtained results. The results of this study are shown in Table 1.

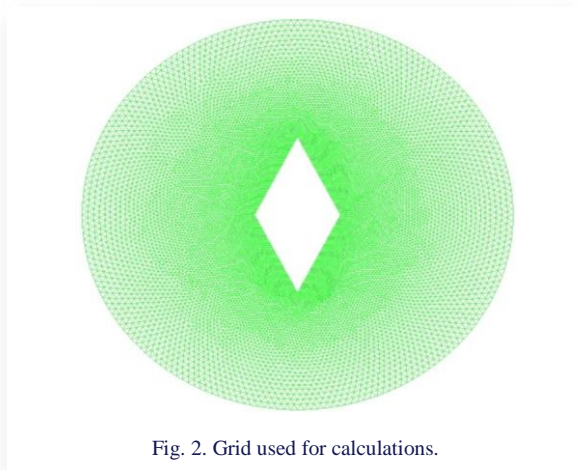


Fig. 2. Grid used for calculations.

As for the numerical solving, it was done by using the finite volumes method of the numerical simulator ANSYS-CFX (14.5). The relative errors of computations were  $10^{-8}$  for the continuity and momentum equations and  $10^{-6}$  for the energy equation. The SIMPLEC algorithm was selected for pressure-velocity coupling. On the other hand, a high-resolution scheme was selected for solving the convective terms of the governing equations.

The accuracy of this method of calculation was verified by

Table 1. Grid independency test for  $Re = 20$ ,  $Ri = 1$  and  $n = 1.4$ .

Mesh	Element	Nu	Difference %
M1	4 956	1.21901	2.10
M2	9 912	1.19343	0.10
M3	19 824	1,19219	0.003
M4	39 648	1,19215	-

Table 2. Validation test for  $Re = 10$  and  $Ri = 3$ .

$n$	Nu [36]	Nu (Present data)	Error %
0.6	3.15324	3.15114	0.066
1.0	2.61236	2.61134	0.040
1.6	1.41546	1.41411	0.095

comparing our results with the previous results of Laidoudi and Ameer [36]. The results of this comparison are shown in Table 2. We note a strong match between the results.

## 5. Results and discussion

This work presents the results of the numerical simulation of a complex fluid trapped between two cylinders. The inner cylinder is cold while the outer one is hot and rotates at a constant and uniform speed. The aim of this study is to know how the heat transfer rate between the fluid and the inner cylinder alters under the influence of the rotational speed of the outer cylinder and the thermal buoyancy force. We mention here that the studied points are:

- The rheological nature of the fluid that changes with the value of the power-law number ( $n$ ).

- The value of the rotational speed of the outer space. The speed of rotation increases with increasing value of Reynolds number.
- The intensity of thermal buoyancy effect. Indeed, the value of this intensity increases with the increasing value of the Richardson number.

Before starting to analyze the results, it is worth remembering that if the thermal buoyancy force is present, the cold spots of the fluid become denser, and this causes them to move to the lower side. Furthermore, the method of displaying the results of this research is similar to the previous methods such as [43–45].

Figure 3 shows the development of the streamlines in terms of  $Re$  and  $n$  at  $Ri = 0$ . In this case, there is no effect of buoyancy (pure forced convection). The movement of the fluid flow is only due to the rotation of the outer enclosure. Since the cylinder is circular, the movement of the flow within the space is also circular. With the inner cylinder acting as an obstacle, steady vortices appear behind the obstacle. It is clear that the size of these zones increases gradually with  $Re$ . Furthermore, there is no significant effect of streamlines with respect to power-law number ( $n$ ). In general, it is noted that the fluid velocity is larger near the outer cylinder, while the velocity decreases gradually as we move towards the inner cylinder.

Figure 4 presents the same developments of the streamlines but with the effect of buoyancy force ( $Ri = 1$ ). It is noticed that the effect of thermal buoyancy affects the three values of ( $n$ ). It is also noted that with the presence of the thermal effect the vortex on the right develops positively, while the vortex on the left develops negatively. On the right-hand side, the movement of the cold fluid spots near the obstacle is opposite to the rotational motion, while on the left-hand side, it is in the same rotation direction of the outer cylinder. From here it is clear that there is an effect of the studied parameters on the heat transfer, which is analyzed later.

Figure 5 presents the contours of dimensionless temperature (isotherms) versus  $Re$  and  $n$  at  $Ri = 0$ . It is clear that there is a degradation of dimensionless temperature. The maximum value of the temperature is near the outer enclosure, and the lower value is around the inner cylinder. Through this distribution, we can know the distribution of temperature gradient in terms of the studied parameters. Through Fig. 5, it is clear that there is a change in the distribution of dimensionless temperature in terms of  $Re$  and  $n$ , especially around the inner cylinder.

Figure 6 shows the same developments of isotherms for the case of  $Ri = 1$ . In this case, the fluid is subjected to the movement as results from two main factors, namely, the rotational movement of the outer cylinder, as well as the cold spots becoming heavier, and this causes them to move downwards. Figure 6 also indicates the variation of temperature gradient in terms of  $Ri$ ,  $Re$  and  $n$ . In addition to this, Fig. 6 shows the circulating motion of the fluid as a result of the circular tail of the isotherms at the bottom of the inner obstacle.

Figure 7 represents the change in the mean value of the Nusselt number in terms of the studied elements ( $Re$ ,  $n$  and  $Ri$ ). In general, the higher the rotational speed of the outer container ( $Re$ ), the higher the value of  $Nu$  in both cases of  $Ri$ . Furthermore,

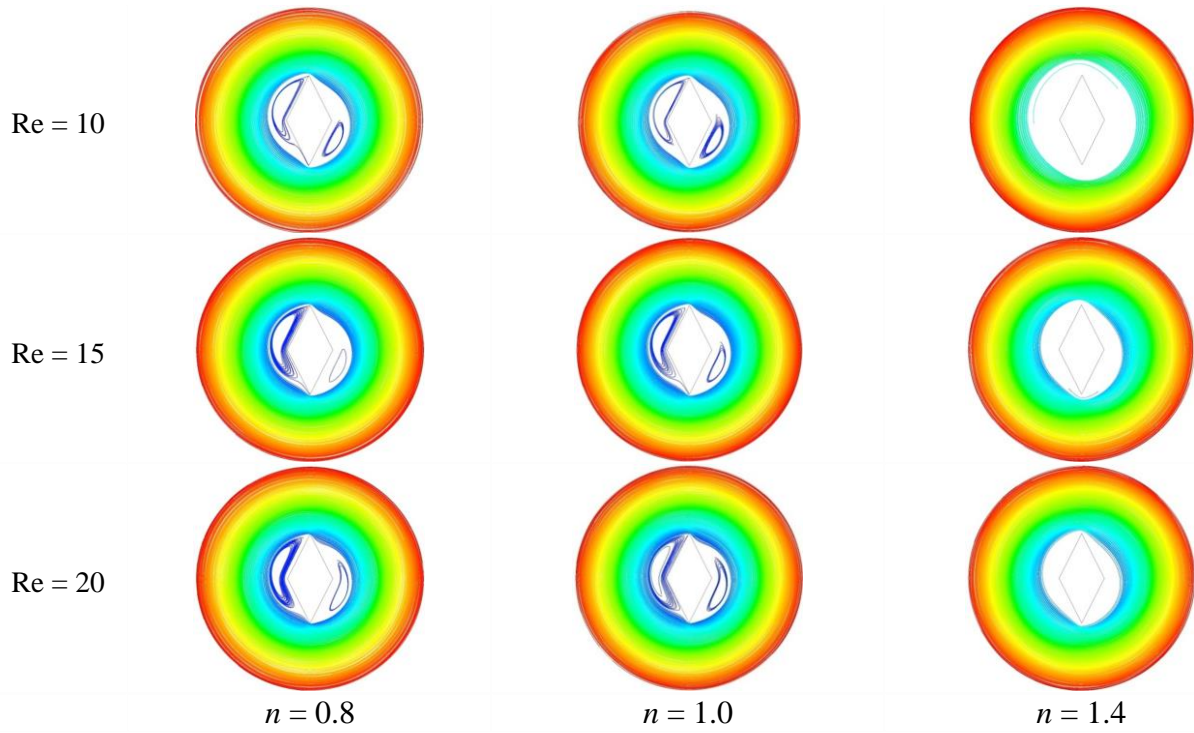


Fig. 3. Streamlines inside the studied domain in terms of Re and  $n$  at  $Ri = 0$ .

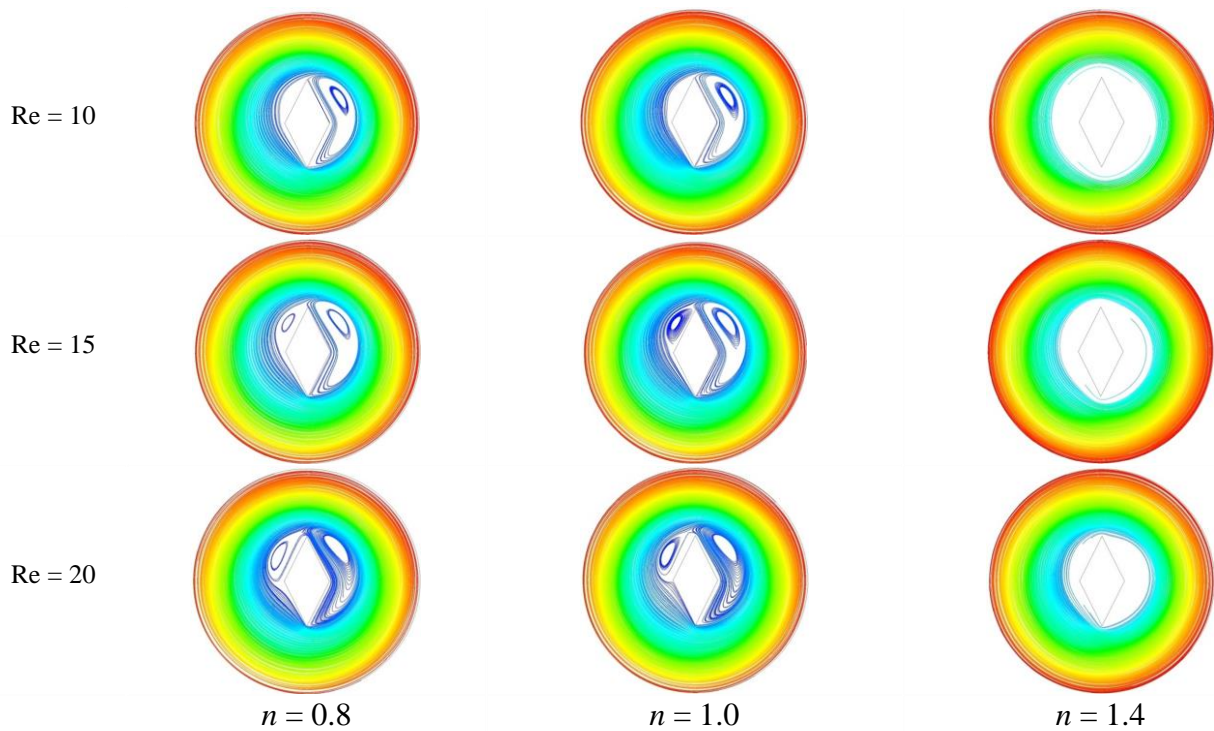


Fig. 4. Streamlines inside the studied domain in terms of Re and  $n$  at  $Ri = 1$ .

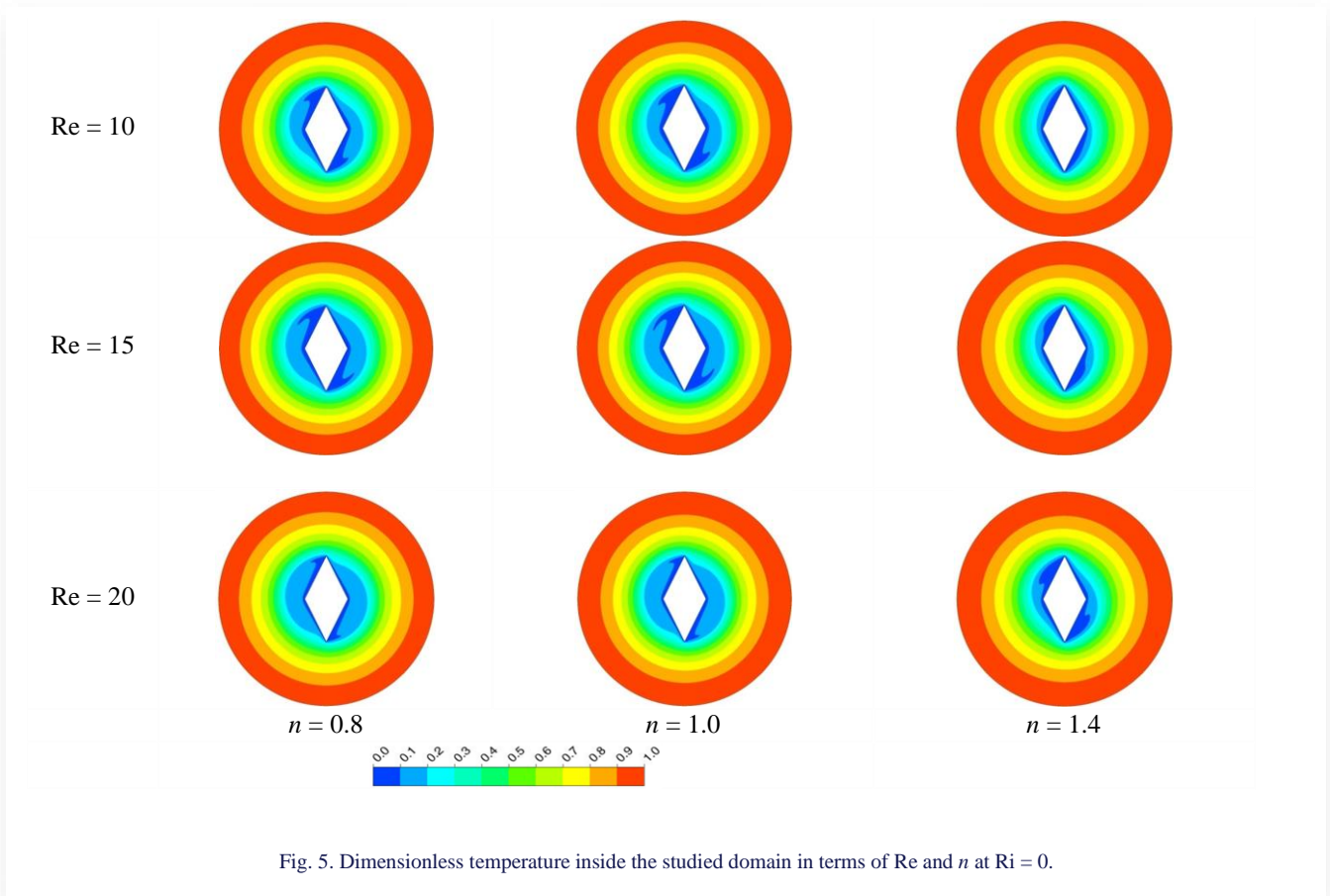


Fig. 5. Dimensionless temperature inside the studied domain in terms of  $Re$  and  $n$  at  $Ri = 0$ .

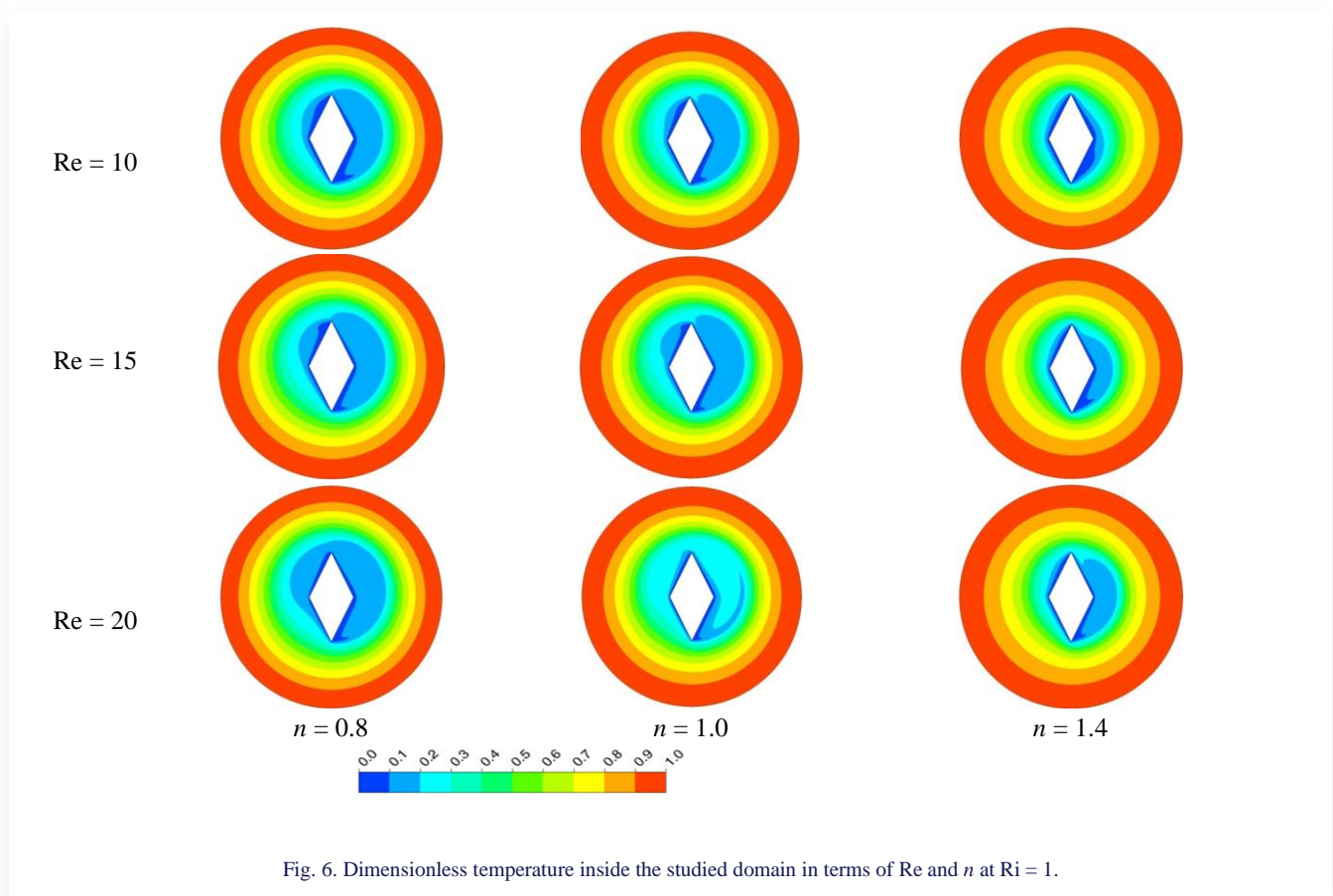


Fig. 6. Dimensionless temperature inside the studied domain in terms of  $Re$  and  $n$  at  $Ri = 1$ .

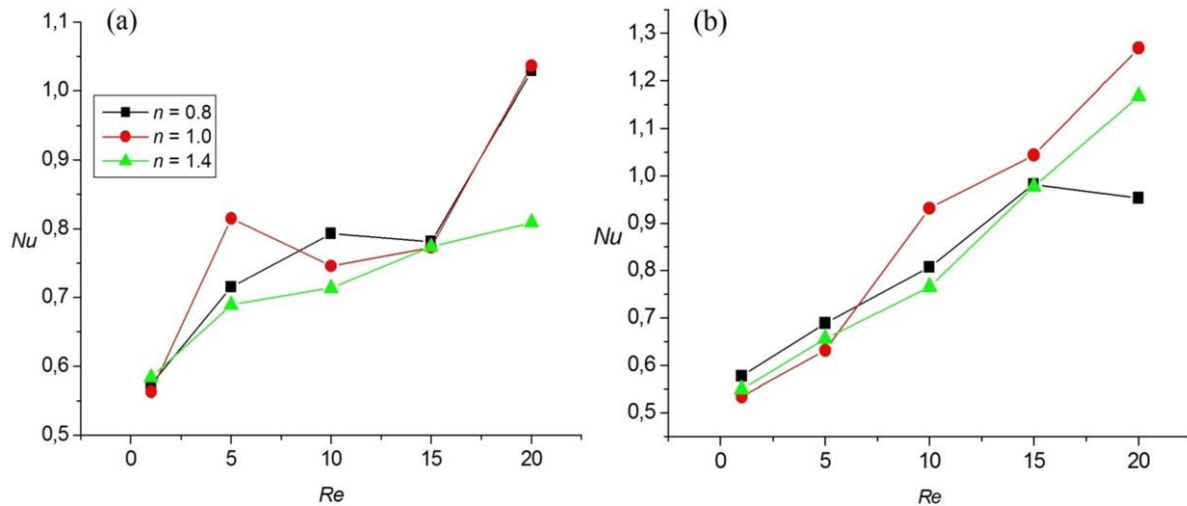


Fig. 7. Variation of Nu versus Re and n; (a) for Ri = 0. (b) for Ri = 1.

it is also noted that the increase of the value of  $n$  decreases the average value of Nu. This is explained as follows: for  $n = 1.4$  this means that the nature of the fluid is complex (shear-thickening fluid). That is, the higher the flow velocity, the higher the dynamic viscosity value, and this dampens the movement of particles of the fluid, making the heat transfer slower. On the contrary, when  $n = 0.8$  the fluid is shear-thinning. The viscosity of the fluid decreases with increasing the velocity of the flow, making the heat transfer faster. Finally, it can be concluded that the fluid being of shear-thickening type impedes heat transfer, making it more effective in thermal insulation applications.

## 5. Conclusions

A set of numerical simulations was achieved in order to study the thermal transfer between obstacles of different shape, temperature and stability pattern. Three types of fluids, whose effects on heat transfer were compared, are, in order: shear-thinning ( $n = 0.8$ ); Newtonian ( $n = 1$ ) and shear thickening ( $n = 1.4$ ). The outer enclosure is also subjected to a circular motion. The effect of thermal buoyancy also was taken into account. Through our study of all these elements, we reached the following points:

- The heat transfer of the inner cylinder increases with the increase in the value of the rotational speed and thermal buoyancy.
- The study showed the presence of two vortices attached to the inner obstacle, the first on the right side and the other on the left side.
- The use of shear-thickening fluid is very effective in applications that include thermal insulation.

For future research related to this topic, we propose to include the influence of the magnetic field on this system with different angles of applications.

## References

- [1] Chatterjee, D., & Halder, P. (2014). MHD mixed convective transport in square enclosure with two rotating circular cylinders. *Numerical Heat Transfer, Part A*, 65(8), 802–824. doi: 10.1080/10407782.2013.846687
- [2] Chatterjee, D., & Halder, P. (2016). Magnetoconvective transport in a lid-driven square enclosure with two rotating circular cylinders. *Heat Transfer Engineering*, 37(2), 198–209. doi: 10.1080/01457632.2015.1044416
- [3] Yoon, H.S., Ha, M.Y., Kim, B.S., & Yu, D.H. (2009). Effect of the position of a circular cylinder in a square enclosure on natural convection at Rayleigh number of  $10^7$ . *Physics of Fluids*, 21(4), 047101. doi: 10.1063/1.3112735
- [4] Terekhov, V.I., & Ekaid, A.L. (2015). Turbulent natural convection inside a parallelepiped with heating of two opposite vertical walls. *High Temperature*, 53(3), 396–405. doi: 10.1134/S0018151X15020236
- [5] Liao, C.C., & Lin, C.A. (2014). Transitions of natural convection flows in a square enclosure with a heated circular cylinder. *Applied Thermal Engineering*, 72(1), 41–47. doi: 10.1016/j.applthermaleng.2014.02.071
- [6] Laidoudi, H., Helmaoui, M., Bouzit, M., & Ghenaïm, A. (2021). Natural convection of Newtonian fluids between two concentric cylinders of a special cross-sectional form. *Thermal Science*, 25(5B), 3701–3714. doi: 10.2298/TSCI200201190L
- [7] Laidoudi, H. (2020). The role of concave walls of inner cylinder on natural convection in annular space. *Acta Mechanica Malaysia*, 3(2), 24–28. doi: 10.26480/amm.02.2020.24.28
- [8] Laidoudi, H. (2020). Natural convection from four circular cylinders in across arrangement within horizontal annular space. *Acta Mechanica et Automatica*, 14(2), 98–102. doi: 10.2478/ama-2020-0014
- [9] Laidoudi, H. (2020). Enhancement of natural convection heat transfer in concentric annular space using inclined elliptical cylinder. *Journal of Naval Architecture and Marine Engineering*, 17(2), 89–99. doi: 10.3329/jname.v17i2.44991
- [10] Masoumi, H., Aghighi, M.S., Ammar, A., & Nourbakhsh, A. (2019). Laminar natural convection of yield stress fluids in annular spaces between concentric cylinders. *International Journal*

- of *Heat and Mass Transfer*, 138, 1188–1198. doi: 10.1016/j.ijheatmasstransfer.2019.04.092
- [11] Tayebi, T., & Chamkha, A.J. (2021). Analysis of the effects of local thermal non-equilibrium (LTNE) on thermo-natural convection in an elliptical annular space separated by a nanofluid-saturated porous sleeve. *International Communications in Heat and Mass Transfer*, 129, 105725. doi:10.1016/j.icheatmasstransfer.2021.105725
- [12] Yigit, S., & Chakraborty, N. (2017). Influences of aspect ratio on natural convection of power-law fluids in cylindrical annular space with differentially heated vertical walls. *Thermal Science and Engineering Progress*, 2, 151–164. doi: 10.1016/j.tsep.2017.05.008
- [13] Chen, S., Liu, Z., Bao, S., & Zheng, C. (2010). Natural convection and entropy generation in a vertically concentric annular space. *International Journal of Thermal Sciences*, 49(12), 2439–2452. doi: 10.1016/j.ijthermalsci.2010.08.011
- [14] Laidoudi, H. (2018). The effect of blockage ratio on fluid flow and heat transfer around a confined square cylinder under the effect thermal buoyancy. *Diffusion Foundations* 16, 1–11. doi: 10.4028/www.scientific.net/DF.16.1
- [15] Cianfrini, M., Corcione, M., & Quintino, A. (2011). Natural convection heat transfer of nanofluids in annular spaces between horizontal concentric cylinders. *Applied Thermal Engineering*, 31(17–18), 4055–4063. doi: 10.1016/j.applthermaleng.2011.08.010
- [16] Helmaoui, M., Laidoudi, H., Belbachir, A., Ayad, A., & Ghaniam, A. (2020). Forced convection heat transfer from a pair of circular cylinders confined in ventilated enclosure. *Diffusion Foundations*, 26, 104–111. doi: 10.4028/www.scientific.net/DF.26.104
- [17] Laidoudi, H., Helmaoui, M., Azeddine, B., Ayad, A. & Ghanaim, A. (2020). Effects of inlet and outlet ports of ventilated square cavity on flow and heat transfer, *Diffusion Foundations*, 26, 78–85. doi: 10.4028/www.scientific.net/DF.26.78
- [18] Hussain, S., Jamal, M., & Ahmed, S.E. (2019). Hydrodynamic forces and heat transfer of nanofluid forced convection flow around a rotating cylinder using finite element method: The impact of nanoparticles. *International Communications in Heat and Mass Transfer*, 108, 104310. doi: 10.1016/j.icheatmasstransfer.2019.104310
- [19] Chatterjee, D., & Mondal, B.(2012). Forced convection heat transfer from an equilateral triangular cylinder at low Reynolds numbers. *Heat and Mass Transfer*, 48(9), 1575–1587. doi: 10.1007/s00231-012-1006-x
- [20] Habib, R.,Yadollahi, B., & Karimi, N. (2020). A Pore-Scale investigation of the transient response of forced convection in porous media to inlet ramp inputs. *Journal of Energy Resources Technologies*, 142(11), 112112. doi: 10.1115/1.4047968
- [21] Alinejad, J., & Esfahani, J. A. (2014). Lattice Boltzmann simulation of forced convection over an electronic board with multiple obstacles, *Heat Transfer Research*, 45(3), 241–262. doi: 10.1615/HeatTransRes.2013005101
- [22] Dey, P., & Das, A. K. (2016). A utilization of GEP (gene expression programming) met model and PSO (particle swarm optimization) tool to predict and optimize the forced convection around a cylinder. *Energy*, 95, 447–458. doi: 10.1016/j.energy.2015.12.021
- [23] Rashidi, S., Dehghan, M., Ellahi, R., Riazee, M., & Jamal-Abad, M.T. (2015). Study of streamwise transverse magnetic fluid flow with heat transfer around an obstacle embedded in a porous medium. *Journal of Magnetism and Magnetic Materials*, 378, 128–137. doi: 10.1016/j.jmmm.2014.11.020
- [24] Gupta, S.K., Ray, S., & Chatterjee, D. (2015). Forced convection heat transfer in power-law fluids around a semi circular cylinder at incidence. *Numerical Heat Transfer, Part A*, 67, 952–971. doi: 10.1080/10407782.2014.955335
- [25] Selimefendigil, F., Öztop, H.F., & Abu-Hamdeh, N. (2020). Impacts of conductive inner L-shaped obstacle and elastic bottom wall on MHD forced convection of a nanofluid in vented cavity. *Journal of Thermal Analysis and Calorimetry*, 141, 465–482. doi: 10.1007/s10973-019-09114-7
- [26] Laidoudi, H., & Makinde, O.D. (2021). Computational study of thermal buoyancy from two confined cylinders within a square enclosure with single inlet and outlet ports. *Heat Transfer*, 50(2), 1335–1350. doi: 10.1002/htj.21932
- [27] Ramla, M., Laidoudi, H., & Bouzit, M. (2022). Behaviour of a non-Newtonian fluid in a helical tube under the influence of thermal buoyancy. *Acta Mechanica et Automatica*, 16, 111–118. doi: 10.2478/ama-2022-0014
- [28] Laidoudi, H., & Bouzit, M. (2018). The Effect of Reynolds and Prandtl number on flow inside of plan channel of waved bottom wall under mixed convection. *Diffusion Foundations*, 16, 21–29. doi: 10.4028/www.scientific.net/DF.16.21
- [29] Xiong, P.Y., Hamid, A., Iqbal, K., Irfan, M., & Khan, M. (2021). Numerical simulation of mixed convection flow and heat transfer in the lid-driven triangular cavity with different obstacle configurations. *International Communications in Heat and Mass Transfer*, 123, 105202. doi: 10.1016/j.icheatmasstransfer.2021.105202
- [30] Singh, R.J., & Gohil, T.B. (2019). Numerical study of MHD mixed convection flow over a diamond-shaped obstacle using OpenFOAM. *International Journal of Thermal Sciences*, 146(7), 106096. doi: 10.1016/j.ijthermalsci.2019.106096
- [31] Shulepova, E.V., Sheremet, M.A.H., Oztop, F., & Abu-Hamdeh, N. (2020). Mixed convection of Al<sub>2</sub>O<sub>3</sub>-H<sub>2</sub>O nanoliquid in a square chamber with complicated fin. *International Journal of Mechanical Sciences*, 165, 105192. doi: 10.1016/j.ijmecsci.2019.105192
- [32] Ahmed, S.E., Mansour, M.A., Hussein, A.K., Mallikarjuna, B., Almeshaal, M.A., & Kolsi, L. (2019). MHD mixed convection in an inclined cavity containing adiabatic obstacle and filled with Cu-water nanofluid in the presence of the heat generation and partial slip. *Journal of Thermal Analysis and Calorimetry*, 138(2), 1443–1460. doi: 10.1007/s10973-019-08340-3
- [33] Qureshi, M. A., Hussain, S., & Sadiq M.A. (2021). Numerical simulations of MHD mixed convection of hybrid nanofluid flow in a horizontal channel with cavity: Impact on heat transfer and hydrodynamic forces. *Case Studies in Thermal Engineering*, 27, 101321. doi: 10.1016/j.csite.2021.101321
- [34] Fu, C., Rahmani, A., Sukatan, W., Alizadeh, S.M., Zarringhalam, M., Chupradit, S., & Toghraie, D.(2021). Comprehensive investigations of mixed convection of Fe-ethylene-glycol nanofluid inside an enclosure with different obstacles using lattice Boltzmann method. *Scientific Reports*, 11, 20710. doi: 10.1038/s41598-021-00038-7
- [35] Yousefzadeh, S., Rajabi, H., Ghajari, N., Sarafraz, M., Akbari, O.A., & Goodarzi, M. (2020). Numerical investigation of mixed convection heat transfer behaviour of nanofluid in a cavity with different heat transfer areas. *Journal of Thermal Analysis and Calorimetry*, 140(3), 2779–2803. doi: 10.1007/s10973-019-09018-6
- [36] Laidoudi, H., & Ameer, H., (2020). Investigation of the mixed convection of power-law fluids between two horizontal concentric cylinders: Effect of various operating conditions. *Thermal Science and Engineering Progress*, 20, 100731. doi: 10.1016/j.tsep.2020.100731
- [37] Laidoudi, H., & Ameer, H. (2022). Complex fluid flow in annular space under the effects of mixed convection and rotating wall of

- the outer enclosure. *Heat Transfer*, 51(5), 3741–3767. doi: 10.1002/htj.22472.
- [38] Al-Kouz, W., Aissa, A., Shamshuddin, M.D., Obai, Y., Sahnoun, M., Anwar Bég, O., & Toghraie, D. (2021). Heat transfer and entropy generation analysis of water-Fe<sub>3</sub>O<sub>4</sub>/CNT hybrid magnetic nanofluid flow in a trapezoidal wavy enclosure containing porous media with the Galerkin finite element method. *The European Physical Journal Plus*, 136(11), 1184. doi: 10.1140/epjp/s13360-021-02192-3
- [39] Shamshuddin, M.D., Mabood, F., Rajput, G.R., Bég, O.A., & Badruddin, I.A. (2022). Thermo-solutal dual stratified convective magnetized fluid flow from an exponentially stretching Riga plate sensor surface with thermophoresis. *International Communications in Heat and Mass Transfer*, 134(4), 105997. doi: 10.1016/j.icheatmasstransfer.2022.105997
- [40] Shamshuddin, M.D., Ullah Khan, S., Bég, O.A., & Bég, T.A. (2020). Hall current, viscous and Joule heating effects on steady radiative 2-D magneto-power-law polymer dynamics from an exponentially stretching sheet with power-law slip velocity: A numerical study. *Thermal Science and Engineering Progress*, 20, 100732. doi: 10.1016/j.icheatmasstransfer.2022.105997
- [41] Kadir, A., Bég, A.O., El Gendy, M., Bég, T.A., & Shamshuddin, M.D. (2019). Computational fluid dynamic and thermal stress analysis of coatings for high-temperature corrosion protection of aerospace gas turbine blades. *Heat Transfer*, 48(6), 2302–2328. doi: 10.1002/htj.21493
- [42] Anwar Bég, O., Bég, T.A., Karim, I., Khan, M.S., Alam, M.M., Ferdows, M., & Shamshuddin, M.D. (2019). Numerical study of magneto-convective heat and mass transfer from inclined surface with Soret diffusion and heat generation effects: A model for ocean magnetic energy generator fluid dynamics. *Chinese Journal of Physics*, 60, 167–179. doi: 10.1016/j.cjph.2019.05.002
- [43] Błasiak, P., & Pietrowicz, S. (2016). Towards a better understanding of 2D thermal-flow processes in a scraped surface heat exchanger. *International Journal of Heat and Mass Transfer*, 98, 240–256. doi: 10.1016/j.ijheatmasstransfer.2016.03.004
- [44] Aliouane, I., Kaid, N., Ameer, H., & Laidoudi, H. (2021). Investigation of the flow and thermal fields in square enclosures: Rayleigh-Bénard's instabilities of nanofluids. *Thermal Science and Engineering Progress*, 25(2), 100959. doi: 10.1016/j.tsep.2021.100959
- [45] Laidoudi, H., & Bouzit, M. (2017). The effect of asymmetrically confined circular cylinder and opposing buoyancy on fluid flow and heat transfer. *Defect and Diffusion Forum*, 374, 18–28. doi: 10.4028/www.scientific.net/DDF.374.18